A tutorial overview of one experiment: WMAP

During today's talk, WMAP will survey 1/3 of the sky (again).

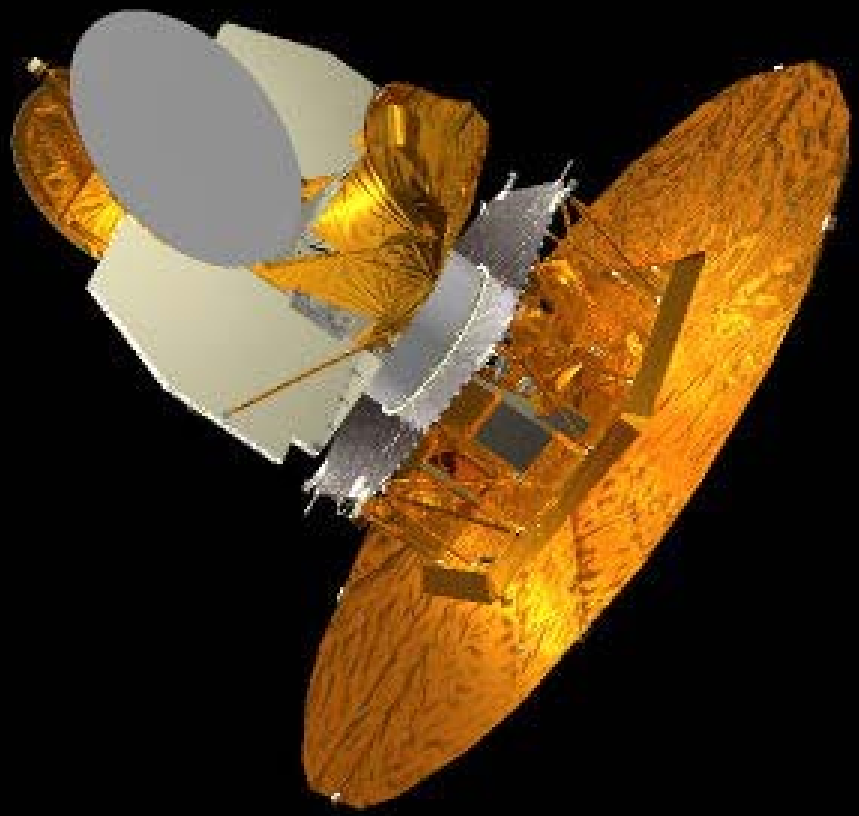

Sun shadow lines

Mark Halpern, UBC

The WMAP Science Team:

C. Bennett (PI)(JHU)
J. Dunkley (Oxford)
B. Gold (JHU)
M. Greason (NASA)
M. Halpern (UBC)
R. Hill (NASA)
G. Hinshaw(NASA)
N. Jarosik (Princeton)
A. Kogut (NASA)
E. Komatsu (UTexas)
D. Larson (JHU)
M. Limon (Columbia)
S. Meyer (Chicago)
M. Nolta (CITA)
N. Odegard (NASA)
L. Page (Princeton)
D. Spergel (Princeton)
G. Tucker (Brown)
J. Weiland (NASA)
E. Wollack (NASA)
E. Wright (UCLA)

…and thanks to WMAP ‘graduates’ C. Barnes, R. Bean, O. Dore, H. Peiris, L. Verde, and especially to David Wilkinson!

•Choose a mature technology--no inventions needed to make WMAP work. It was 5 years from proposal to launch.

•Focus on aspects of the experiment which MUST be done on a satellite.

•No cryogenics or active thermal control.

•Make the full data pipeline early in the project, and use it to understand the impact on our systematic error budget of all design decisions.

•Have a very small science team so that everyone talks to everyone.

WMAP was designed to produce all sky maps with the following properties:

- 0.2 degree angular resolution
- Accuracy on all scales above 0.2 degrees
- Minimally correlated pixel noise
- Polarization sensitivity
- Calibration accuracy <0.5%
- Sensitivity levels <20μK for 393,216 sky pixels
- Systematic errors < 5% of random variance on all angular scales.

These goals lead to a design with:

•A symmetric differential instrument

•Rapid large sky-area scans

•Several (4) switching/modulation periods

•Interconnected redundant observations

•An L2 orbit to minimize sun/moon/earth effects and provide thermal stability

•Sidelobe response which keeps the Sun/Moon/Earth below 1 μK

•Five bands to allow separation of galactic and cosmic signals

•Passive thermal control and a constant sun angle

• Calibration in flight based on the CMB dipole and its annual modulation by WMAP's orbit, and

•Precision temperature sensing of the instrument.

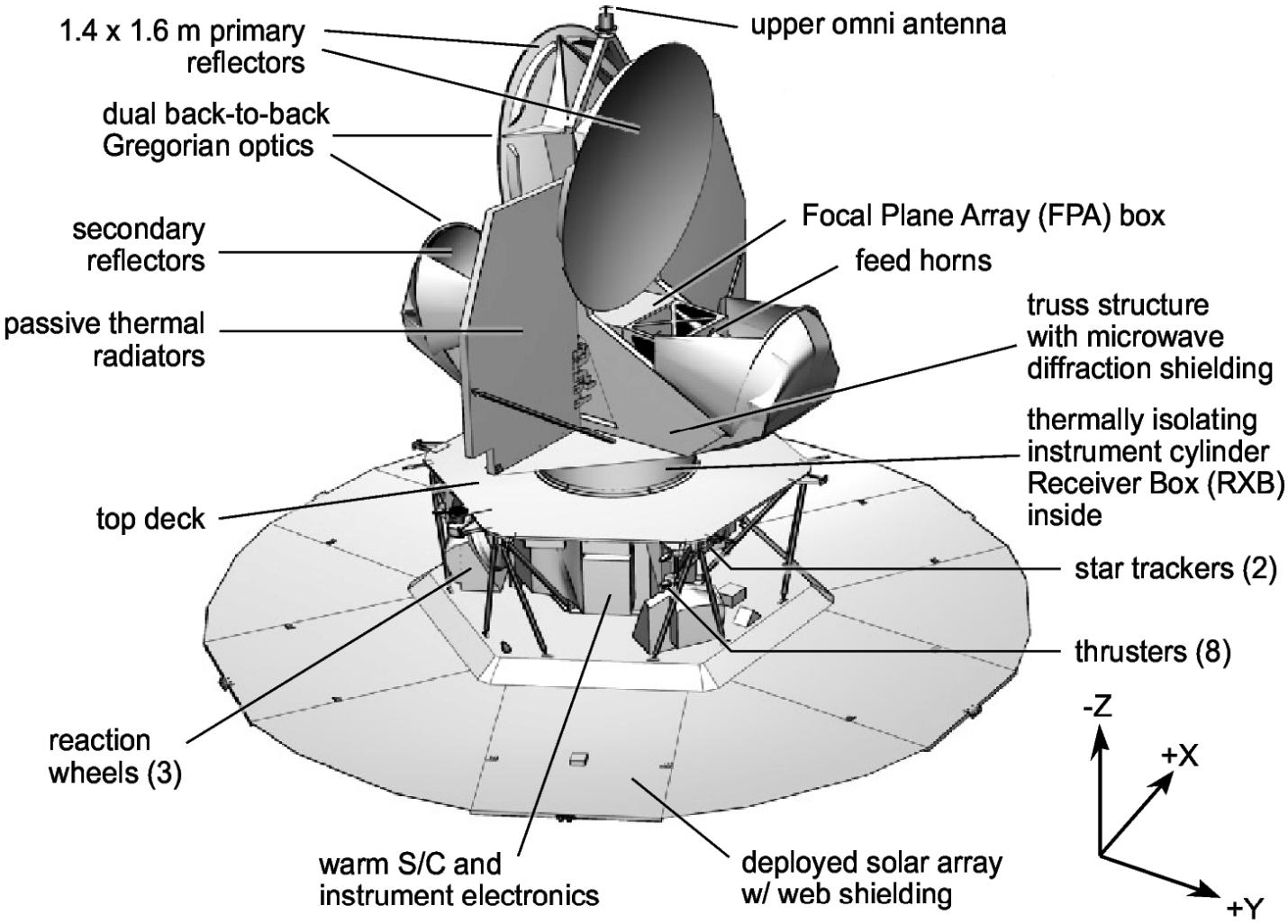

Figure 1.1: Spacecraft Overview. View of the spacecraft in the deployed configuration with major components labeled. The primary and secondary reflectors as well as the two thermal radiators are clearly visible in the upper portion of the image. The cold and warm section of the radiometers are housed in the FPA and RXB respectively and are locate in the core of the spacecraft under the primary reflectors. All the support electronics (AEU, DEU, PDU, MAC, LMAC), gyros, star-trackers, and reactions wheels are mounted on the hexagonal hub at the base of the spacecraft. While at L2, the optics, instrument and support electronics are constantly in the shade of the solar array and never exposed to solar radiation.

Table 1. Approximate Observational Properties by Band

Item	K-Band	Ka-Band	Q-Band	V-Band	W-Band
Wavelength, λ (mm)	13	9.1	7.3	4.9	3.2
Frequency, ν (GHz)	22.8	33.0	40.7	60.8	93.5
Ant./therm. conversion factor, $\Delta T/\Delta T_A$	1.014	1.029	1.044	1.100	1.251
Noise, σ_0 (mK) $\sigma = \sigma_0 N_{obs}^{-1/2}$	1.424	1.449	2.211	3.112	6.498
Beam width θ(°FWHM)	0.82	0.62	0.49	0.33	0.21
No. of Differencing Assemblies	1	1	2	2	4
No. of Radiometers	2	2	4	4	8
No. of Channels	4	4	8	8	16

The WMAP frequency bands were chosen to lie near the minimum in foreground contamination and to provide enough frequency coverage and resolution to recognize and remove galactic emission.

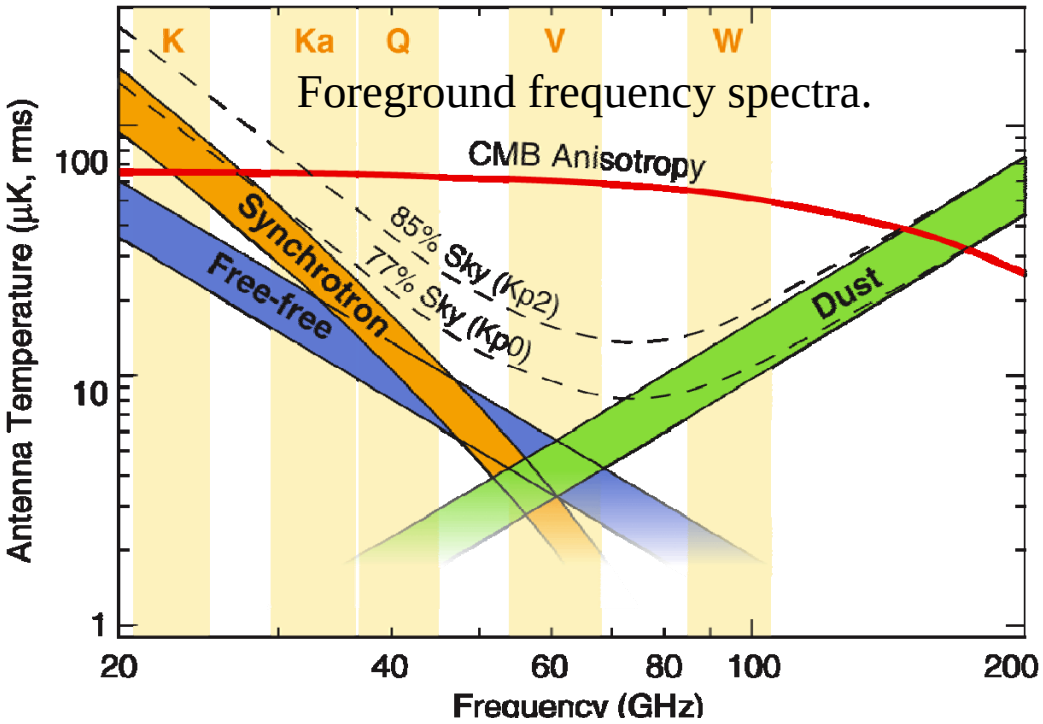

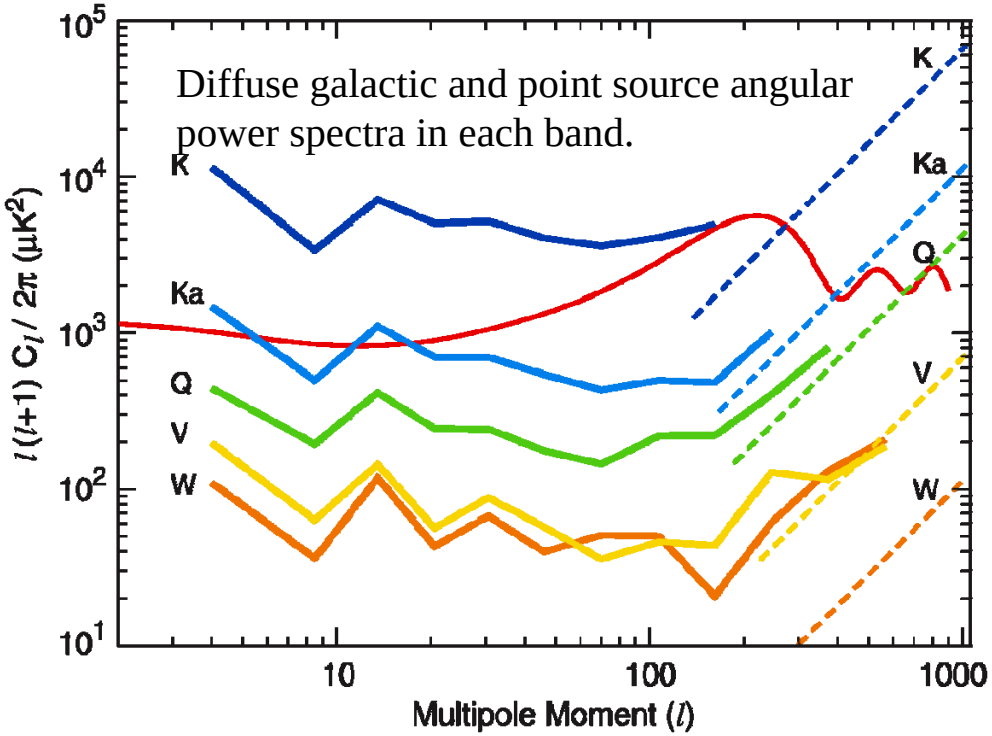

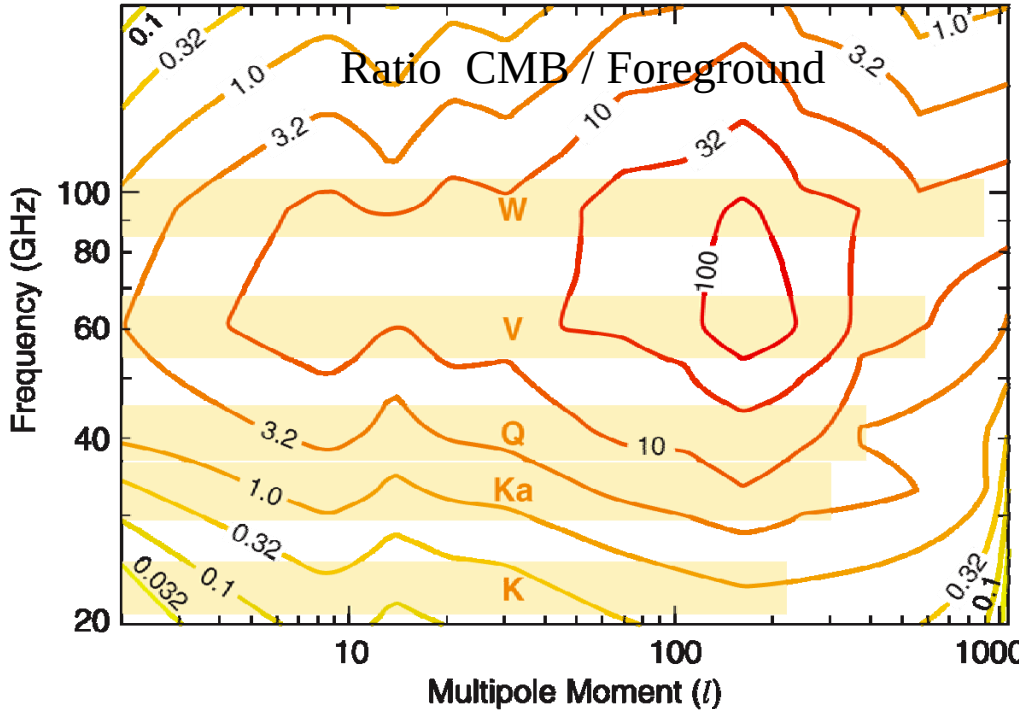

WMAP with mm resolution and km resolution:

Goddard snapshot

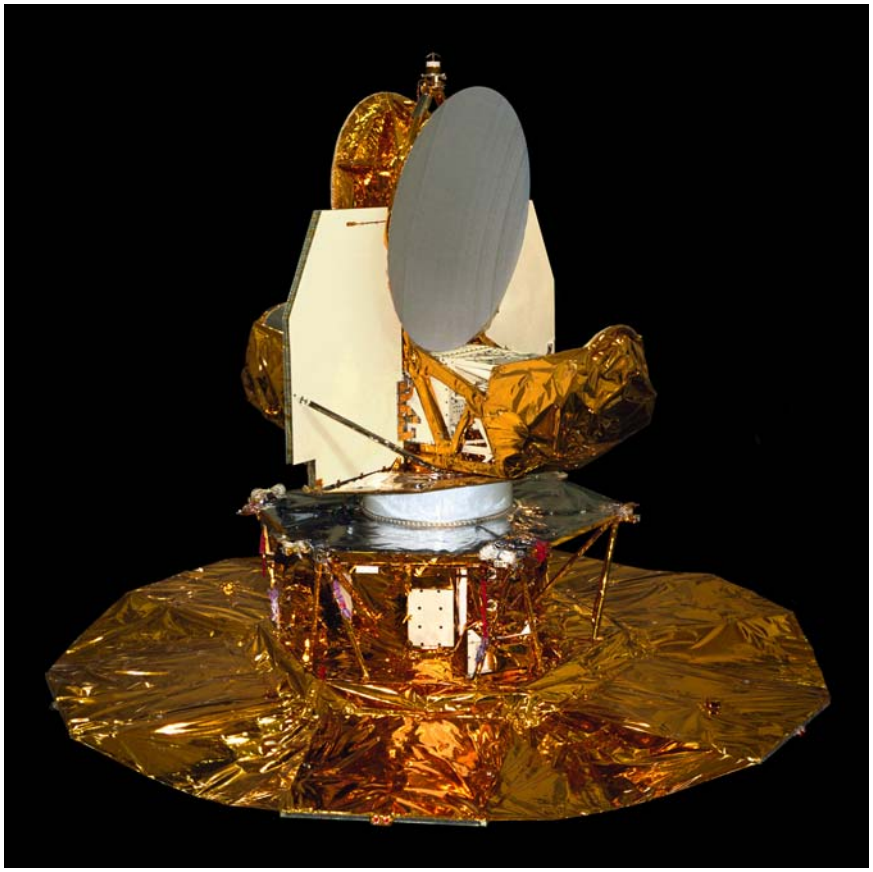

WMAP is a very symmetric differential instrument with sufficient frequency coverage and resolution to understand foreground emission.

CHFT Image

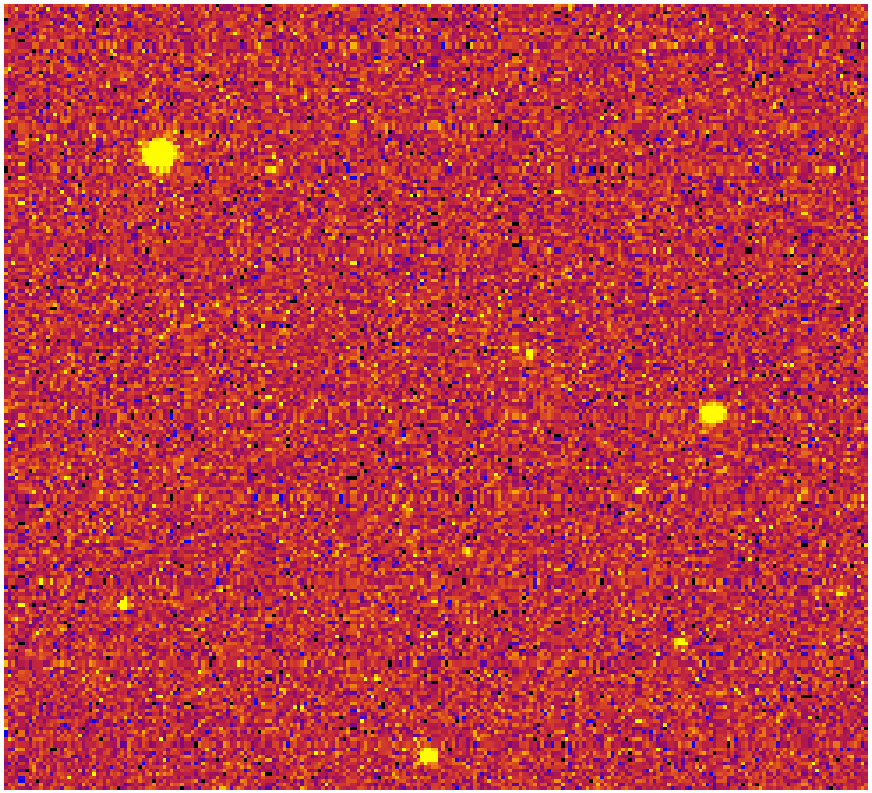

WMAP observes the sky from L2. The environment is very stable, and the sun, moon and earth never enter the field of view.

(3 10s exposures on CFHT, August 2001)

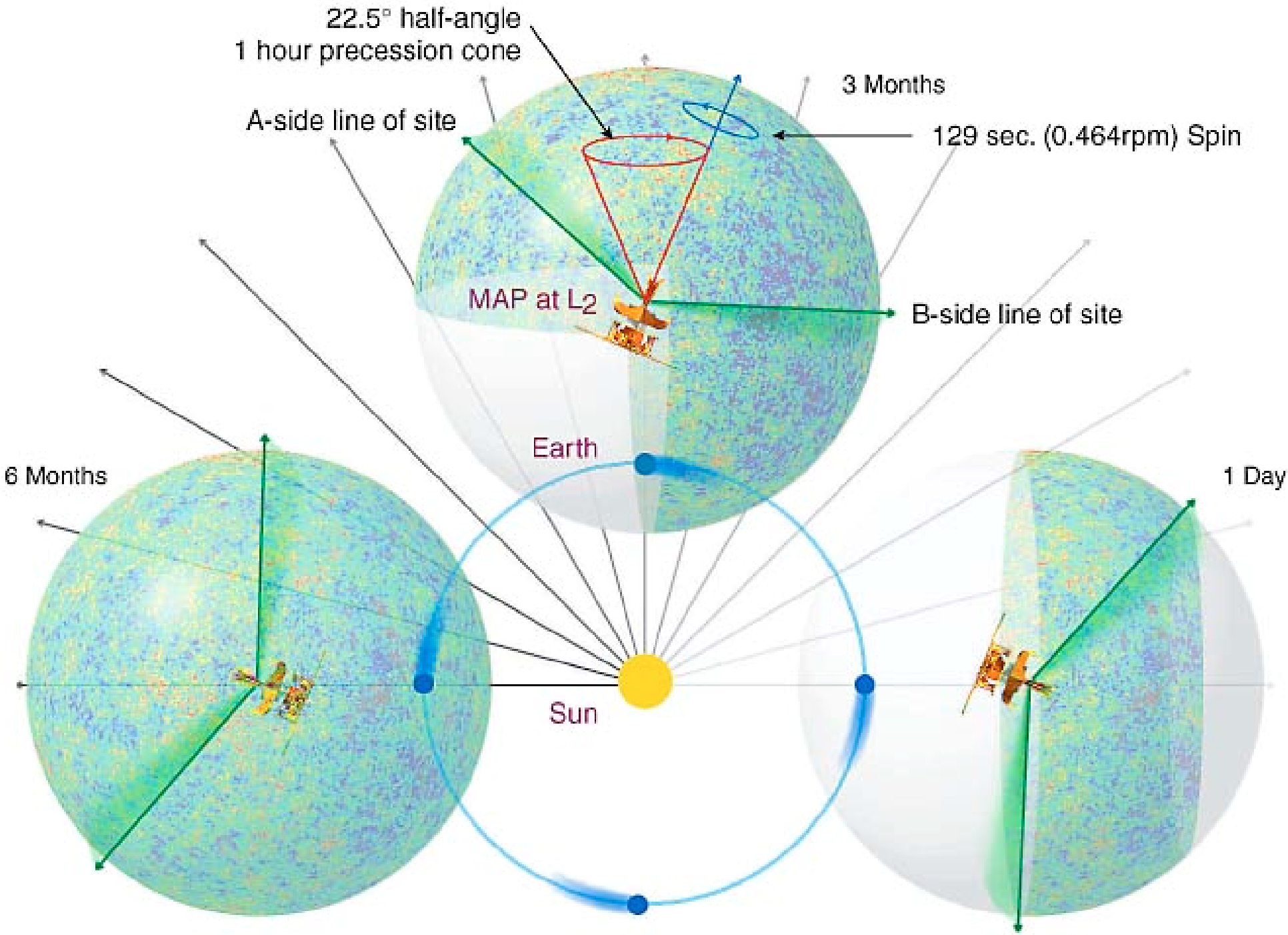
22.5° half-angle
1 hour precession cone
A-side line of site
3 Months
129 sec. (0.464rpm) Spin
MAP at L2
B-side line of site
Earth
6 Months
1 Day
Sun

The whole sky is shown in Equatorial coordinates with the WMAP observation pattern in white. The scan pattern covers 30% of the sky every hour, and every circular scan of the sky crosses all the others providing interconnections at many angular scales.

This is achieved with a fixed angle between the spacecraft axis and the sun!

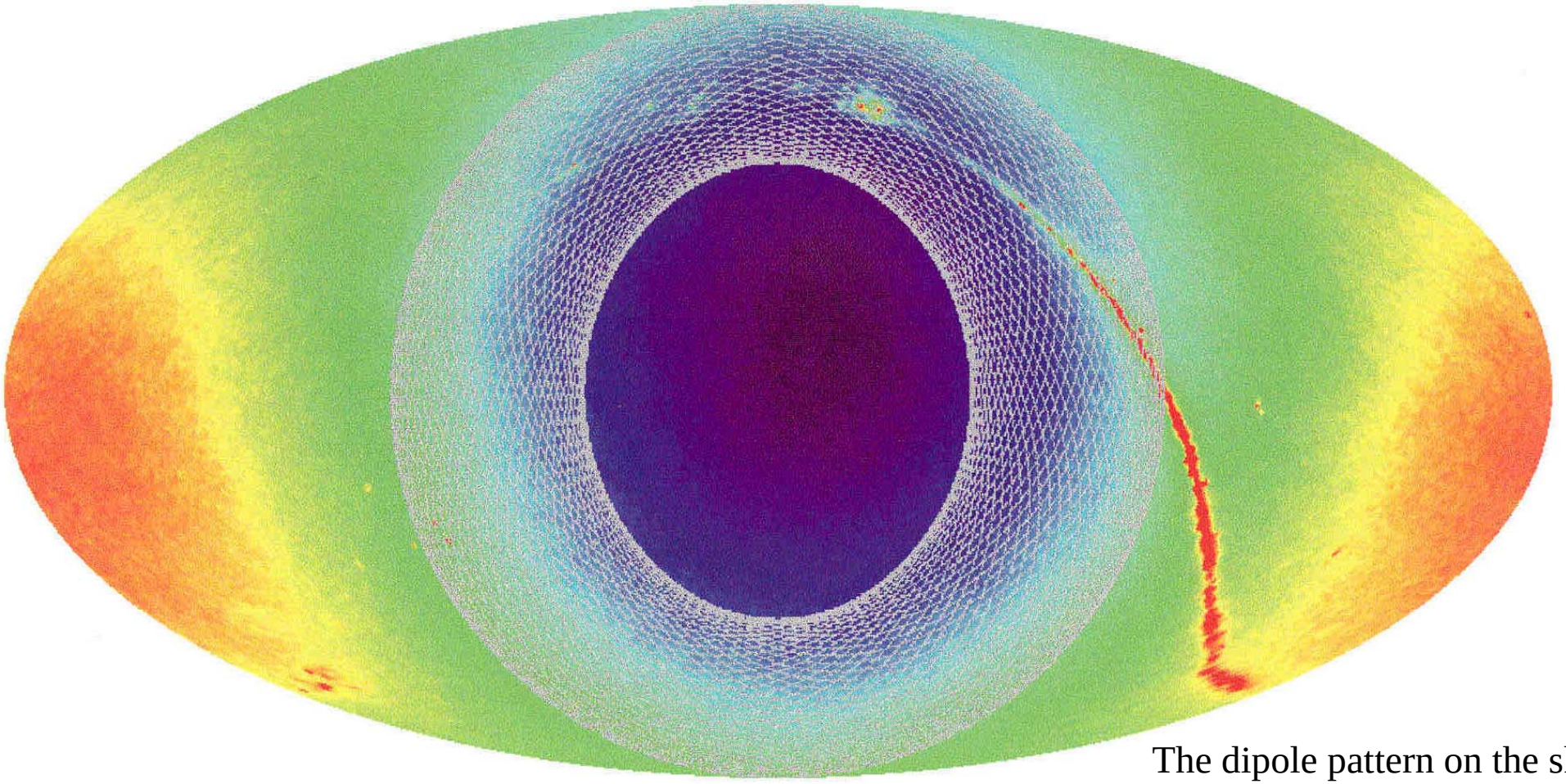

The dipole pattern on the sky arises because the solar system is not at rest w.r.t the expansion of the universe.

WMAP Time Ordered Data

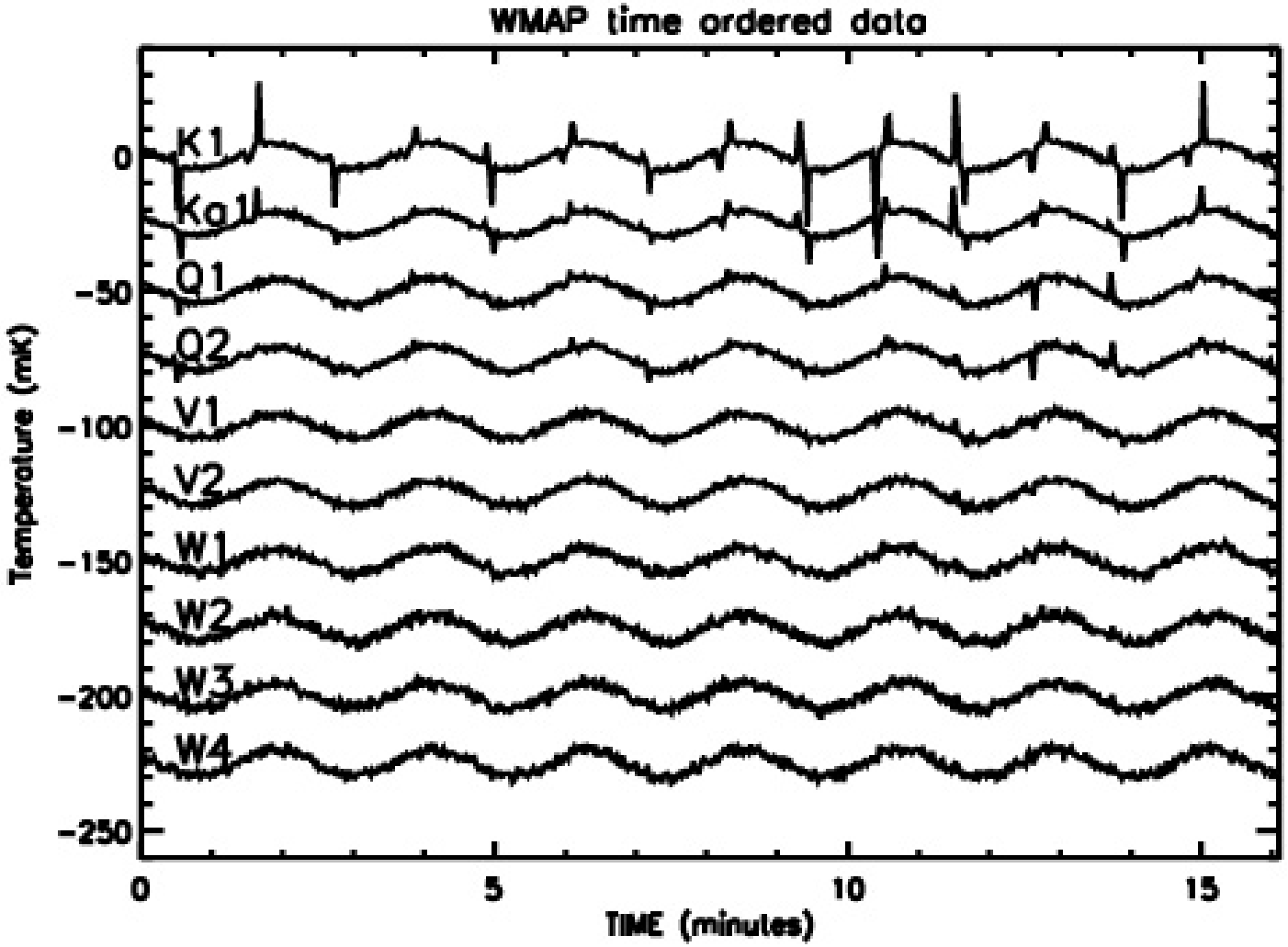

The CMB dipole provides an hourly calibration monitor.

Ultimate calibration is derived from the annual variation in the dipole as the spacecraft orbits the sun. Precision is 0.5%.

Sky Map Iterations #0, 1, and 10

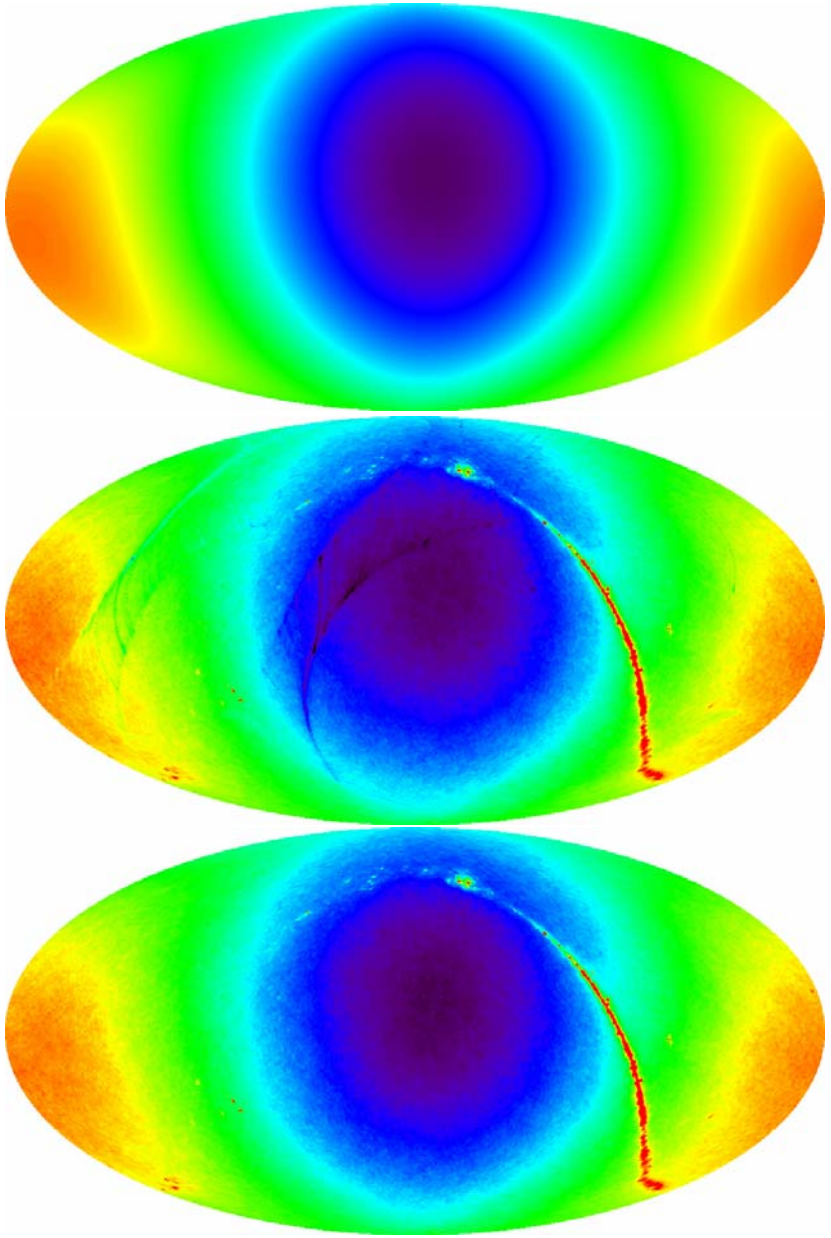

Initial guess of sky temperature:
$t^{(0)}$ = pure dipole

Response after 1 iteration -
note spurious “Galaxy echos”

Response after 10 iterations -
excellent convergence

Maps are inferred from the data by iterative deconvolution. The gain is determined from the CMB dipole in the same process.

Hourly gain inferred from the cmb dipole amplitude.

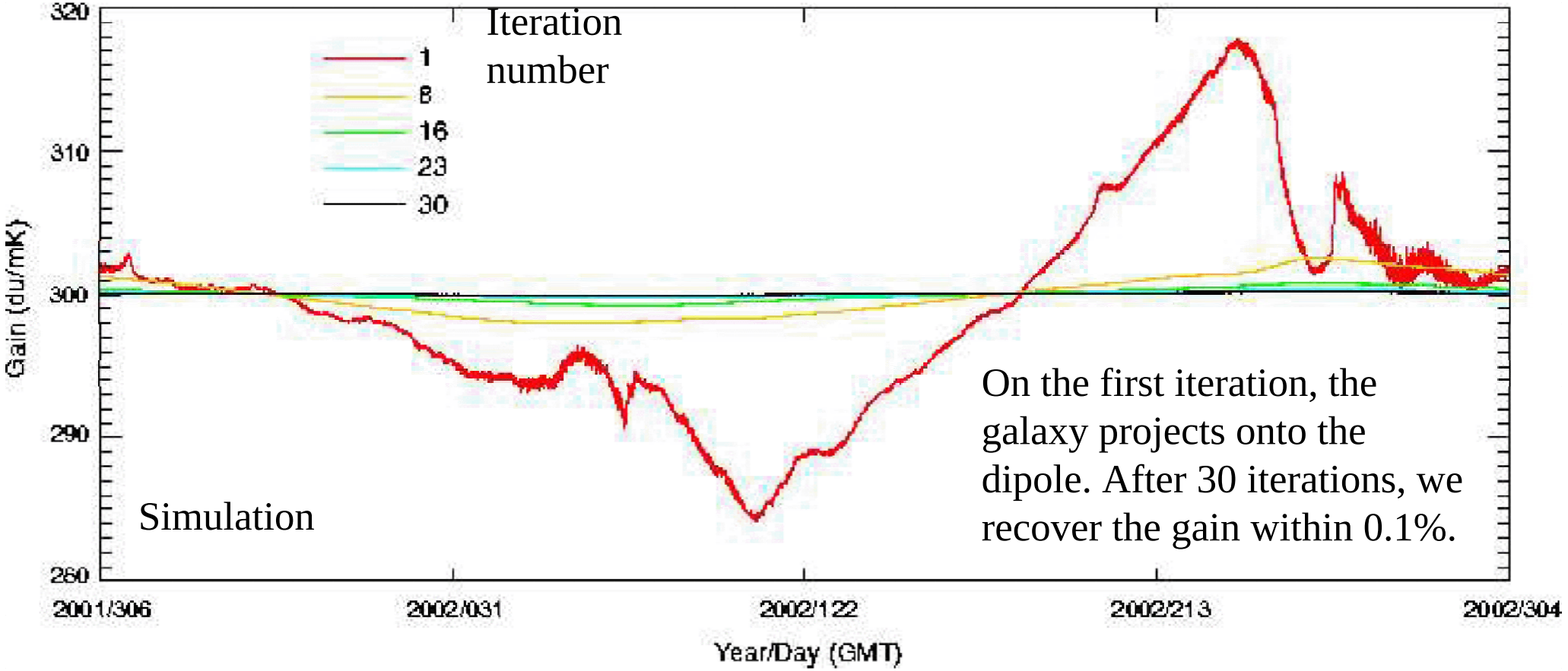

Ultimately, the experiment is calibrated against the *annual change* in the CMB dipole caused by the earth's orbital motion around the sun.

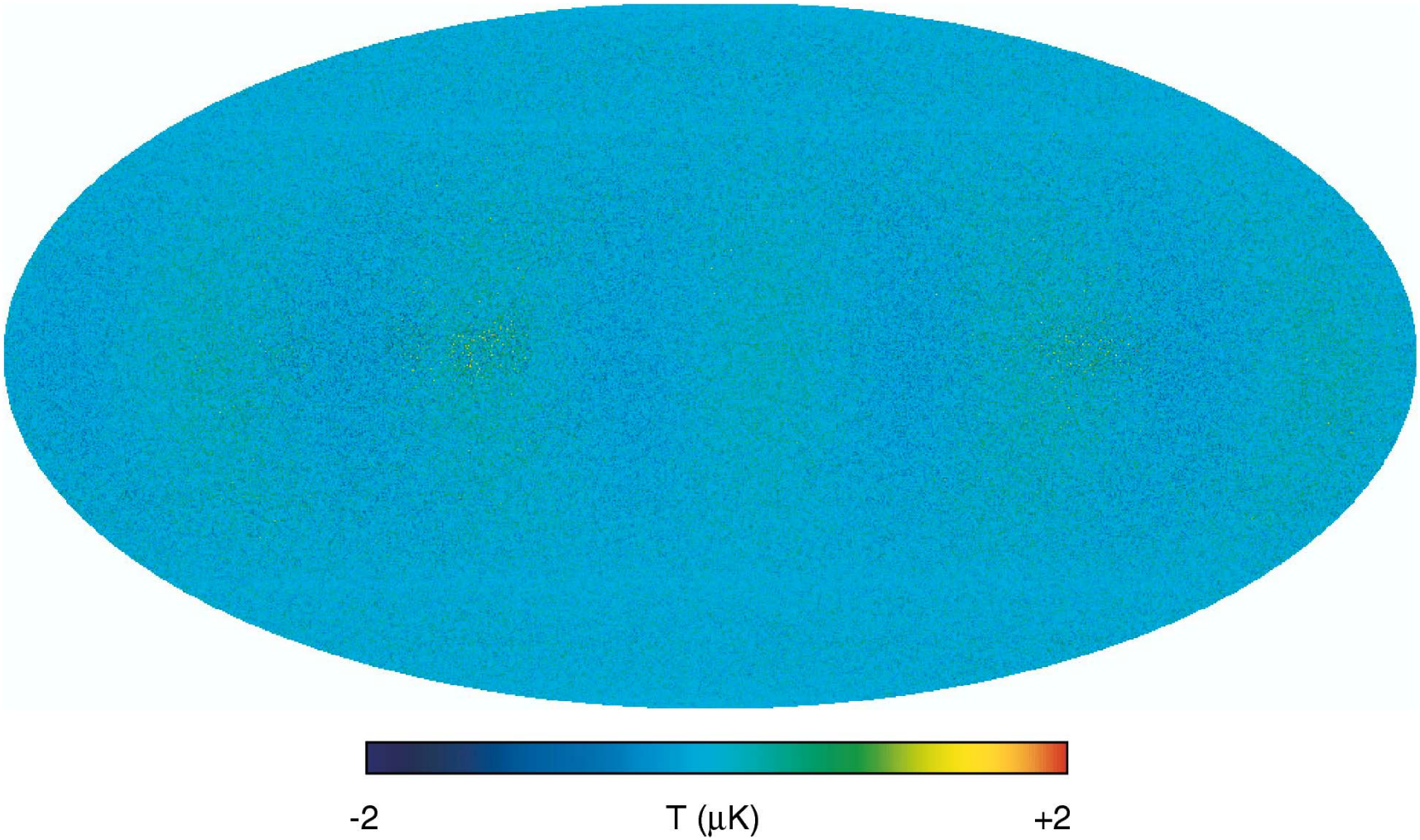

Fig. 1.— A residual sky map, $\mathbf{t}_{\rm out} - \mathbf{t}_{\rm in}$, from an "ideal" one-year simulation of Q2 data, designed to test the iterative map-making algorithm presented in §2.1. The input sky map included realistic CMB signal with a peak-to-peak amplitude of $\sim \pm 420$ μK, and a Galactic signal with a peak brightness of $\sim$50 mK. The rms structure in this map is $<$0.2 μK, after accounting for the 0.15 μK noise ($\sim$ 2 du in the time-ordered data) that was introduced to the simulation to dither the digitized signal. The map is projected in ecliptic coordinates and shows the anisotropy mode that is least well measured by *WMAP*, due to a combination of the scan pattern and the beam separation angle. This residual level is the result of 50 iterations of the algorithm – more iterations would reduce it even further.

Table 5. Calibration and Map-Making Error Limits[a]

DA	C_2 (μK^2)	$\langle C_l \rangle_{3-10}$ (μK^2)	$\langle C_l \rangle_{11-100}$ (μK^2)	$\sigma^{sys}\|_2$ (μK^2)	$\sigma^{sys}\|_{3-10}$ (μK^2)	$\sigma^{sys}\|_{11-100}$ (μK^2)
K1	-21.4	0.6	0.08	42.9	1.1	0.03
Ka1	18.5	1.3	0.06	37.0	2.5	0.01
Q1	59.6	1.2	0.14	118.9	2.2	0.01
Q2	7.3	0.9	0.13	14.4	1.6	0.02
V1	3.9	0.6	0.21	7.4	0.7	0.01
V2	-6.1	0.8	0.19	12.6	1.2	0.03
W1	-2.6	1.4	0.49	6.0	2.0	0.10
W2	12.0	0.7	0.62	22.9	0.4	0.15
W3	4.3	0.4	0.65	7.3	0.4	0.07
W4	-6.6	3.3	0.90	14.5	5.4	0.55

[a]All values derived from a one-year simulation of *WMAP* data. The first 3 data columns give the mean power in the residual map $\mathbf{t}_{\rm out} - \mathbf{t}_{\rm in}$ from the simulation. The last 3 columns give an estimate of the systematic error due to calibration and map-making, as defined in §3.1. For comparison, the average power in the CMB in each band is $C_2 \sim 130$ μK^2, $\langle C_l \rangle_{3-10} \sim 150$ μK^2, and $\langle C_l \rangle_{11-100} \sim 6$ μK^2.

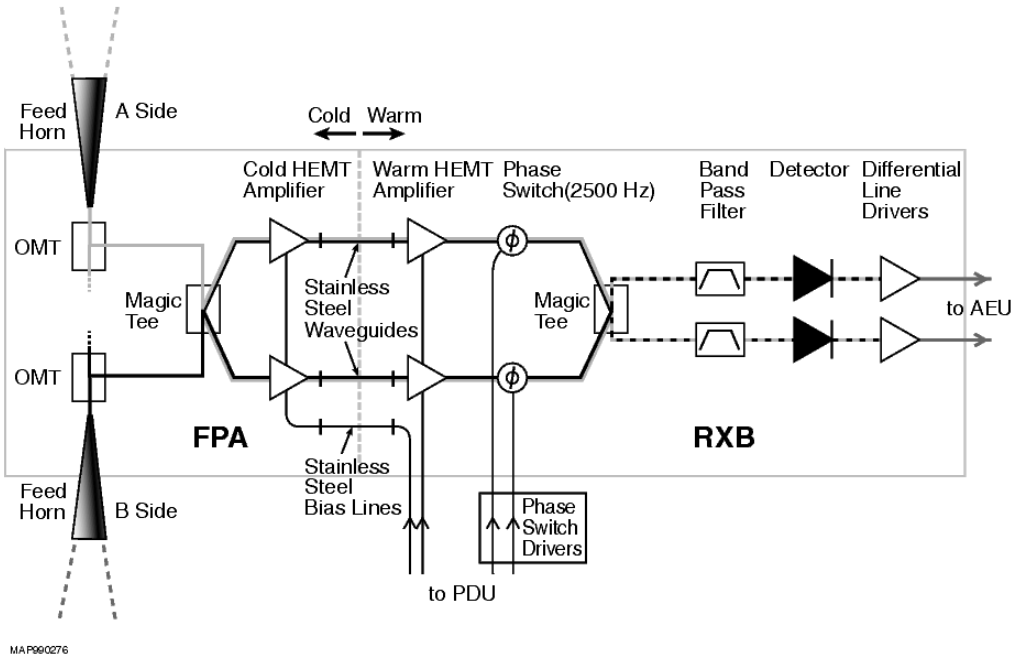

Figure 1.2: Layout of an Individual *WMAP* Radiometer. Components on the cold (left) side of the stainless steel waveguides are housed in the FPA where they passively cooled to ~ 90 K through thermal links to the radiator panels. The components in the RXB achieve a balance temperature of ~ 290 K.

We test additive and multiplicative systematic errors form every stage in the system by moving temperatures of each component up and down while looking at stable cold thermal loads before flight.

WMAP systematic errors are measured in flight to be very small.

Spin synchronous systematic errors would accumulate in the maps.

Notice the upper limits for these effects are measured in nano-Kelvin.

Limits on Spin-Synchronous Environmental Effects[a]

Radiometer/ Band	Gain nK	Thermal nK	Voltage nK
K	6.2	27	4.8
Ka	0.8	2	4.6
Q	15.9	2	7.0
V	0.3	77	37.4
W	0.1	173	9.9

[a] 1σ upper limits derived from measured gain and baseline susceptibilities in Table 8, combined with upper limits on temperature and voltage fluctuations at the spin period. Sign is preserved for each radiometer for roll-up by band.

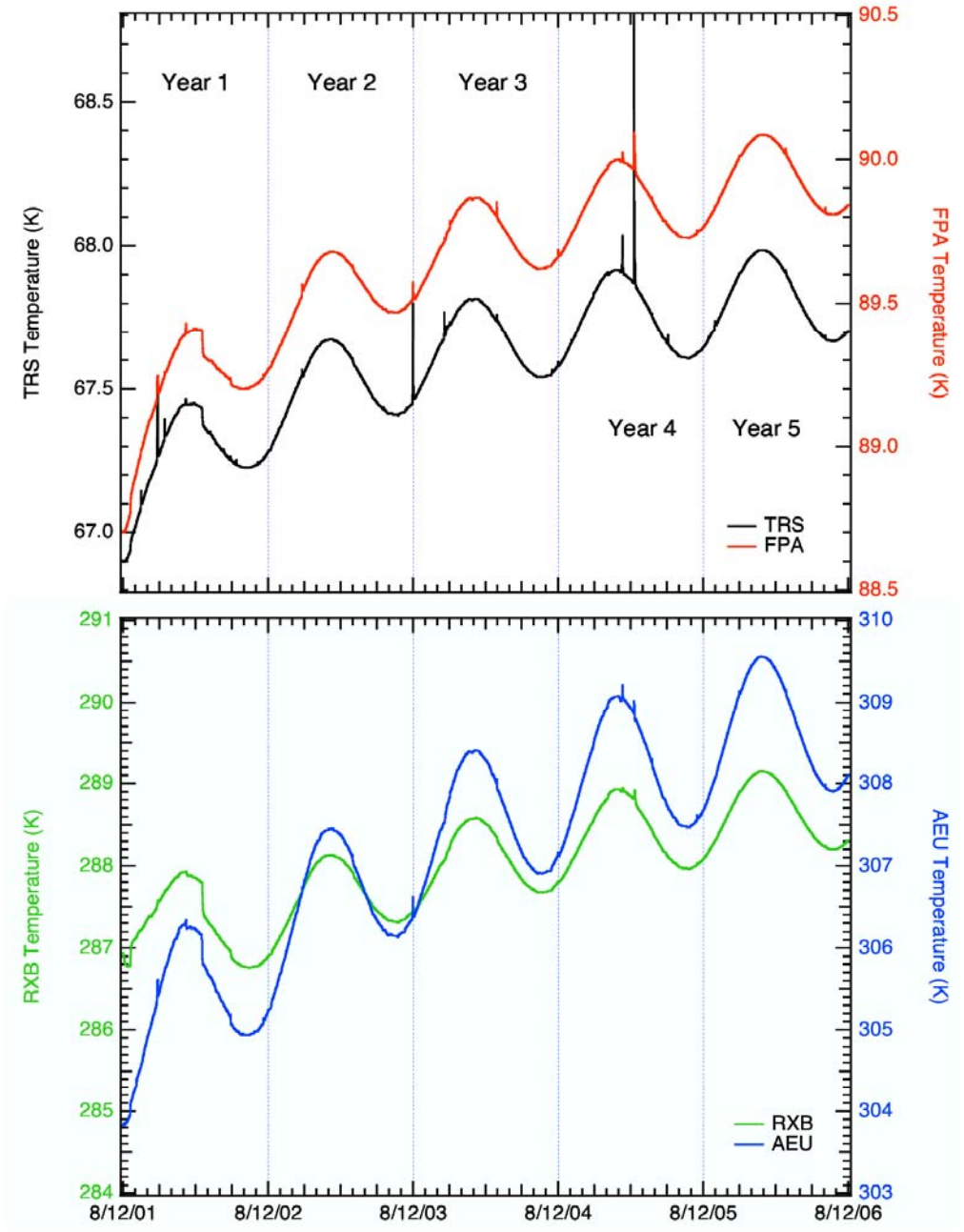

Figure 1.6: Five Years Thermal Profile. The measured thermal profile for the cumulative five years of operation covers 2001:222 (08/10/2001) to 2006:222 (08/10/2006). Expanded plots and details are shown in Figures 1.7, 1.8, 1.9, 1.10 and 1.11.

Continued Thermal Stability

The pattern of the 200 micro K variation of our primary mirrors has not changed over the three years indicating that the observatory thermal environment remains excellent. (The few 100 nK optical signal this variation produces does not sum to a signal in the map due to WMAP's symmetrized observation strategy.)

Rotation-averaged mirror-temperature variations over three years.

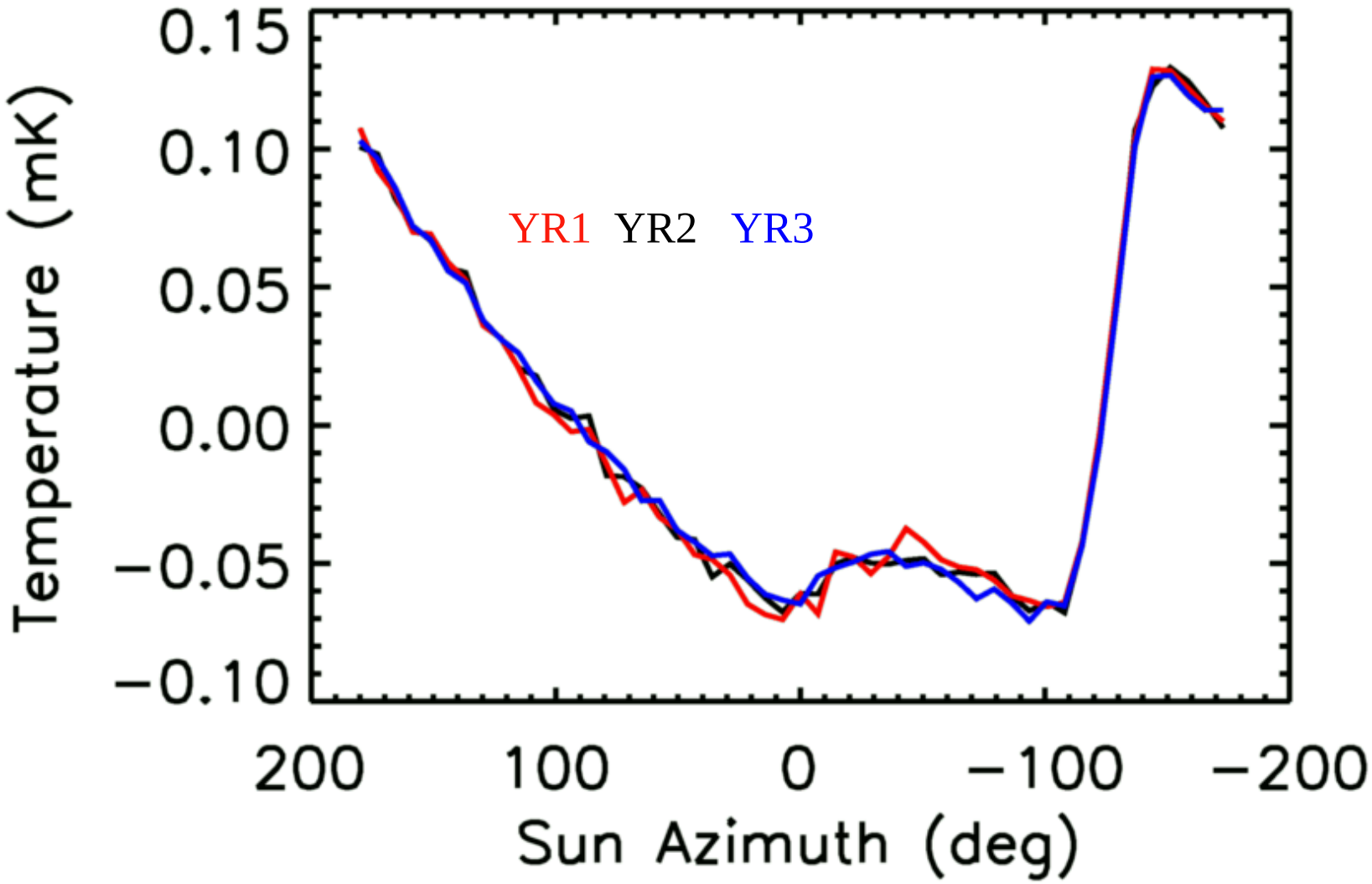

The brightest parts of the galactic plane are 1000 times brighter than the CMB.

However, the WMAP far sidelobe response is so low that the average pickup in Q,V and W bands is under 1 micro Kelvin.

Sidelobe contamination levels for unpolarized microwave sky maps.

DA	Mean (μK)	Min (μK)	Max (μK)	rms (μK)	$\ell_{\max}$	$\max(C_\ell)$ (μK^2)
K1	9	-17	72	15	6	30
Ka1	2	-1.6	9	2	6	0.4
Q1	1.4	-4	10	2	2	4
Q2	1.3	-4	10	2	2	4
V1	0.3	-2×10^{-2}	0.6	0.3	2	3×10^{-2}
V2	0.2	-2×10^{-2}	0.6	0.2	2	2×10^{-2}
W1	-0.12	-1.4	1.0	0.4	4	6×10^{-2}
W2	-6×10^{-2}	-3	3	0.8	4	0.5
W3	-5×10^{-2}	-3	3	0.8	4	0.5
W4	-0.12	-1.4	1.0	0.4	4	8×10^{-2}

We calculate 28 Cross-power spectra (Q1xQ2, Q1xV1, etc but never W2xW2). These 28 measurements of the power spectrum agree, indicating very little galactic contamination.

Here they are shown one *l* per bin. The scatter about a smooth spectrum is due to cosmic variance: there are not enough multipoles in our universe to determine their variance well.

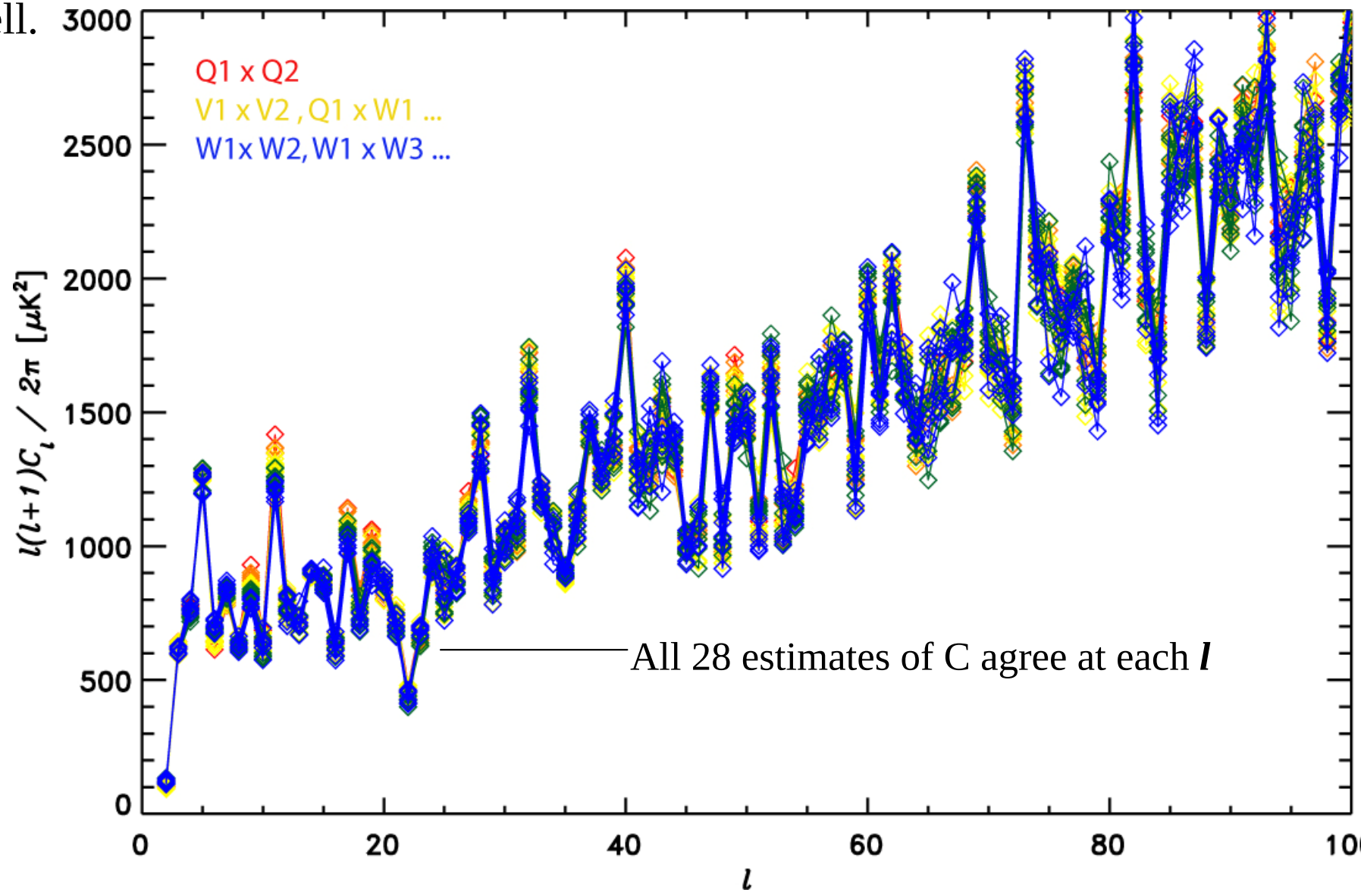

We will need to understand our **beam shapes** very well to understand our maps.

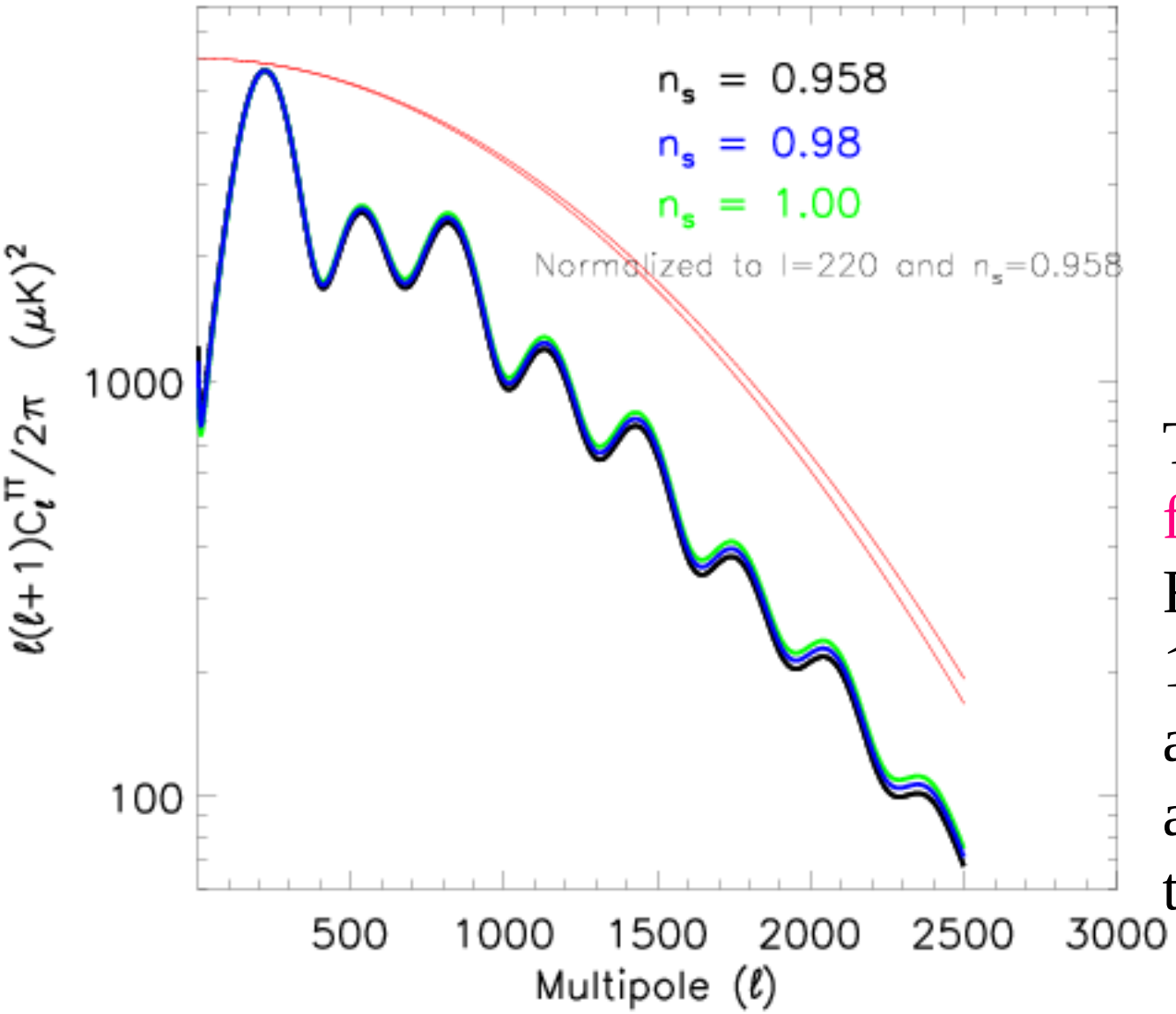

Overall normalization, spectral index, tilt and unscrambling matter densities all rely on knowing our beam area and beam shape to high precision.

The two window functions are for 0.1 deg FWHM beams with a 1% difference in solid angle. Only WMAP has achieved anything like this accuracy.

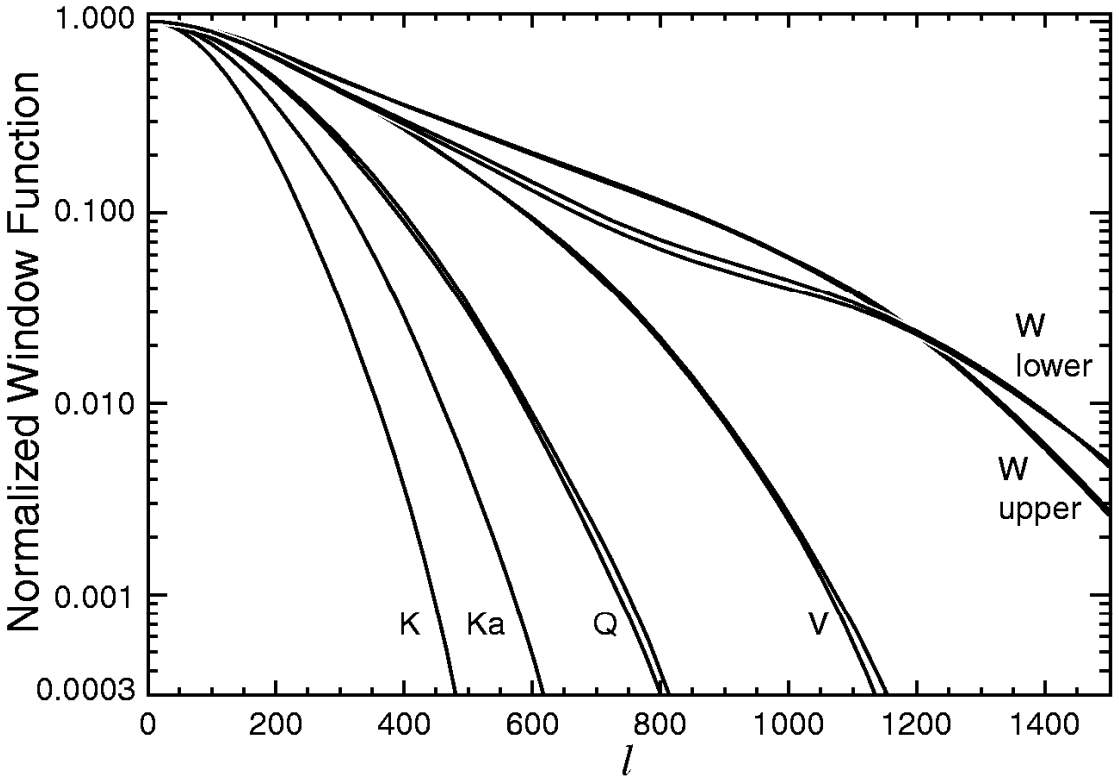

FIG. 4.— The ten window functions, w_l, computed from the Hermite expansion. The window functions for the two polarizations in each feed are the same.

Data used in determining the WMAP beam shapes:

- The main beam shape is determined from in-flight measurements of the response to Jupiter.
- There are pre-launch measurements of the near side lobe response made in the Goddard compact range
- There are far sidelobe measurements made on a rooftop at Princeton
- There are physical measurements made of thermal distortion and motion made at Goddard thermal facilities
- We observed the moon during our trip out to L2

Hill *et al.* 0803.0570

We have more data from Jupiter and better maps of the CMB, which confuse our Jupiter maps.

A major improvement is that we now have high fidelity models of both sides of our optical system. The models let us extend beam integrals beyond the angular range of high S/N Jupiter data.

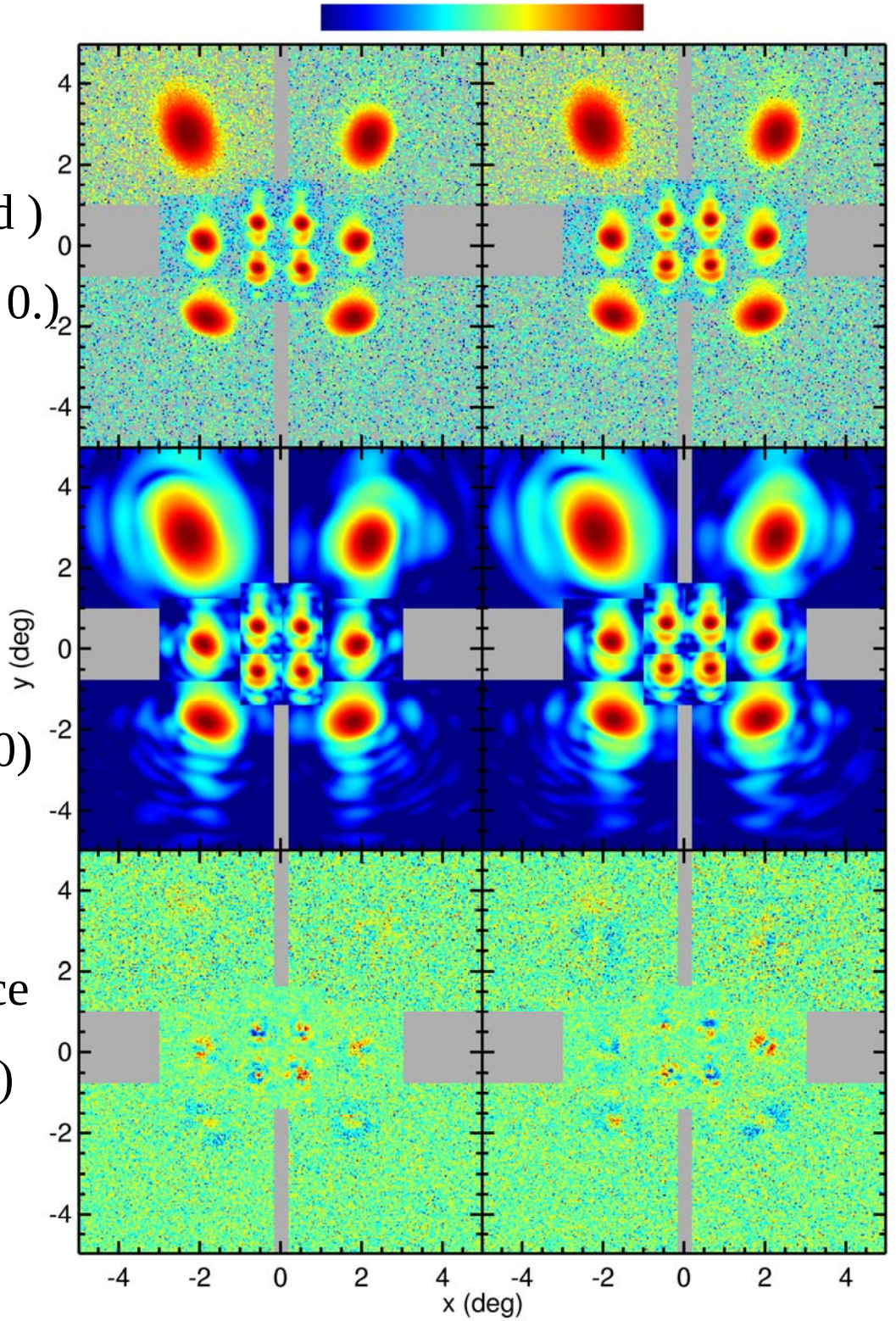

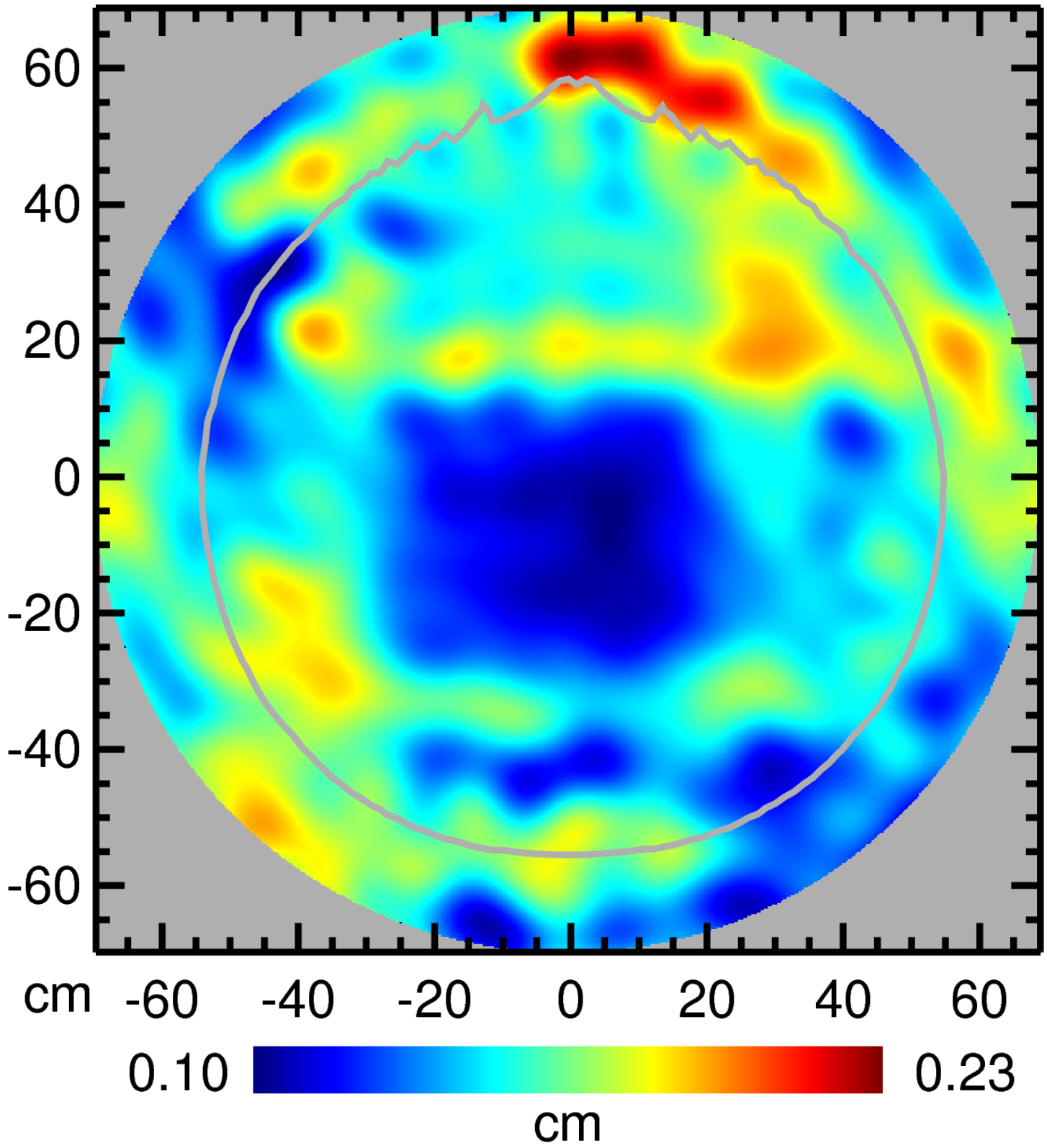
60
40
20
0
-20
-40
-60
cm
-60
-40
-20
0
20
40
60
0.10
0.23
cm

Our beam uncertainties have dropped by almost a factor of two, while the difference between the beam shape we inferred at Yr-3 and Yr-5 is less than the Yr-3 1σ uncertainties.

Notice that the total beam solid angle has gone up for all V and W band by from 0.5% to 1.5%. Much of this change is within the primary beam.

Black: Yr3-Yr5 window functions.

Red: Yr-3 1-σ uncertainties

Hill *et al.* 0803.0570